Articles

Role of Neighboring FMN Side Chains in the Modulation of Flavin Reduction Potentials and in the Energetics of the FMN:Apoprotein Interaction in *Anabaena* Flavodoxin†

Isabel Nogués,‡ Luis Alberto Campos,‡ Javier Sancho,‡ Carlos Gómez-Moreno,‡ Stephen G. Mayhew,§ and Milagros Medina*,‡

Departamento de Bioquímica y Biología Molecular y Celular, Facultad de Ciencias and Institute of Biocomputation and Physics of Complex Systems (BIFI), Universidad de Zaragoza, 50009-Zaragoza, Spain, and Department of Biochemistry, Conway Institute for Biomolecular and Biomedical Research, University College Dublin, Belfield, Dublin 4, Ireland

Received August 5, 2004; Revised Manuscript Received September 23, 2004

ABSTRACT: Flavodoxins (Flds) are electron transfer proteins that carry a noncovalently bound flavin mononucleotide molecule (FMN) as a redox active center. A distinguishing feature of these flavoproteins is the dramatic change in the $E_{sq/rd}$ reduction potential of the FMN upon binding to the apoprotein (at pH 8.0, from −269 mV when free in solution to −438 mV in *Anabaena* Fld). In this study, the contribution of three neighboring FMN residues, Thr56, Asn58, and Asn97, and of three negatively charged surface residues, Glu20, Asp65, and Asp96, to modulate the redox properties of FMN upon its binding to the apoprotein has been investigated. Additionally, the role of these residues in the apoflavodoxin:FMN interaction has been analyzed. Concerning the redox potentials, the most noticeable result was obtained for the Thr56Gly mutant. In this Fld variant, the increased accessibility of FMN leads to an increase of +63 mV in the $E_{sq/rd}$ value. On the other hand, a correlation between the electrostatic environment of FMN and the $E_{sq/rd}$ has been observed. The more positive residues or the less negative residues present in the surroundings of the FMN N(1) atom, then the less negative the value for $E_{sq/rd}$. With regard to FMN binding to apoflavodoxin, breaking of hydrophobic interactions between FMN and residues 56, 58, and 97 seems to increase the K_d values, especially in the Thr56Gly Fld. Such results suggest that the H-bond network in the FMN environment influences the FMN affinity.

Flavodoxins (Flds)[1] are small α/β flavoproteins involved in electron-transfer (ET) reactions in microorganisms and certain algae, which are either constitutively synthesized or induced to replace ferredoxin (Fd) under iron stress conditions. Flds are noncovalent complexes between an apoprotein [apoflavodoxin (ApoFld)] and a low-potential flavin cofactor, the FMN, that confers redox properties to the protein. Binding of ApoFld to FMN modifies the free flavin midpoint reduction potentials, with $E_{ox/sq}$ being displaced to a less negative value, while $E_{sq/rd}$ is shifted to a more negative one (*1*, *2*). These changes reflect a stabilization of the intermediate flavin semiquinone by the protein. The role played by the protein environment in modulating the properties of bound FMN has been studied using Flds from several sources. These studies have demonstrated the importance of electrostatic interactions (*3*−*9*), aromatic stacking interactions (*3*, *10*, *11*), flavin−sulfur interactions (*12*) and H bonds to either flavin N(3) (*13*, *14*) or flavin N(5) (*7*, *15*−*17*).

Three-dimensional structures of a large number of Flds are known in their oxidized state (*18*−*23*), with some structures also known for the corresponding semiquinone and/or hydroquinone states (*2*, *23*−*26*). Structures are also available for mutants of some of these proteins (*9*, *17*, *27*−*29*) and for the ApoFld from *Anabaena* (*30*). Although the overall folding of the polypeptide is similar in all Flds, there is considerable variation in specific interactions between the FMN cofactor and the apoprotein. In general, the isoalloxazine moiety of the flavin is locked in a nonpolar environment and is stacked against at least one aromatic side chain.

† This work has been supported by Comisión Interministerial de Ciencia y Tecnología (CICYT, BQU2001-2520 to M.M. and BCM 2001-252 to J.S.), by DGA (P120/2001 to J.S.) and by a FEBS Travel Grant (to I.N.).

* To whom correspondence should be addressed: Departamento de Bioquímica y Biología Molecular y Celular, Facultad de Ciencias, Universidad de Zaragoza, 50009-Zaragoza, Spain. Phone: 34-976-762-476. Fax: 34-976-762-123. E-mail: mmedina@unizar.es.

‡ Universidad de Zaragoza.

§ University College Dublin.

[1] Abbreviations: dRf, 5-deazariboflavin; dRfH·, semiquinone form of dRf; ET, electron transfer; $E_{ox/sq}$, midpoint reduction potentials for the ox/sq couple; $E_{sq/rd}$, midpoint reduction potentials for the sq/rd couple; WT, wild type; *F*, Faraday's constant; Fld, flavodoxin; ApoFld, apoflavodoxin; Fld_{ox}, Fld in the oxidised state; Fld_{rd}, Fld in the hydroquinone state; Fld_{sq}, Fld in the semiquinone state; K_d, dissociation constant; EPR, continuous wave electron paramagnetic resonance; ESEEM, electron spin−echo envelope modulation.

10.1021/bi0483256 CCC: $27.50
Published on Web 11/06/2004

```
.....................          1.................20//51.................70//80.....................100
Anabaena PCC 7120              SKKIGLFYGTQTGKTESVAE  IIGCPTWNIG--ELQSDWEGLY  GKLVAYFGTGDQIGYADNFQD
Anacystis nidulans             -AKIGLFYGTQTGVTQTIAE  IIGCPTWNVG--ELQSDWEGIY  GKKVAYFGAGDQVGYSDNFQD
Clostridium beijerinckii       ---MKIVYWSGTGNTEKMAE  ILGCSAMGDE-VLEESEFEPFI  GKKVALFGSYGWG-----DGK
Desulfovibrio vulgaris         MPKALIVYGSTTGNTEYTAE  LLGCSTWGDDSIELQDDFIPLF  GRKVACFGCGDSS--YEYFCG
Desulfovibrio desulfuricans    MSKVLILFGSSTGNTESIAQ  LMGCSAWGMEDLELQDDFAPLF  GKKLAAFASGDME--YEHYCG
                                                   *       * *       *                      **
```

FIGURE 1: Sequence alignment of flavodoxins from *Anabaena*, *A. nidualns*, *C. beijerinckii*, *D. vulgaris*, and *D. desulfuricans* at the regions involved in FMN binding among residues 1−20, 51−70, and 80−100. Alignments have been obtained with CLUSTALW. Numeration corresponds to that of *Anabaena* Fld. Residues in bold and presenting an asterisk under sequence are those studied in the present paper.

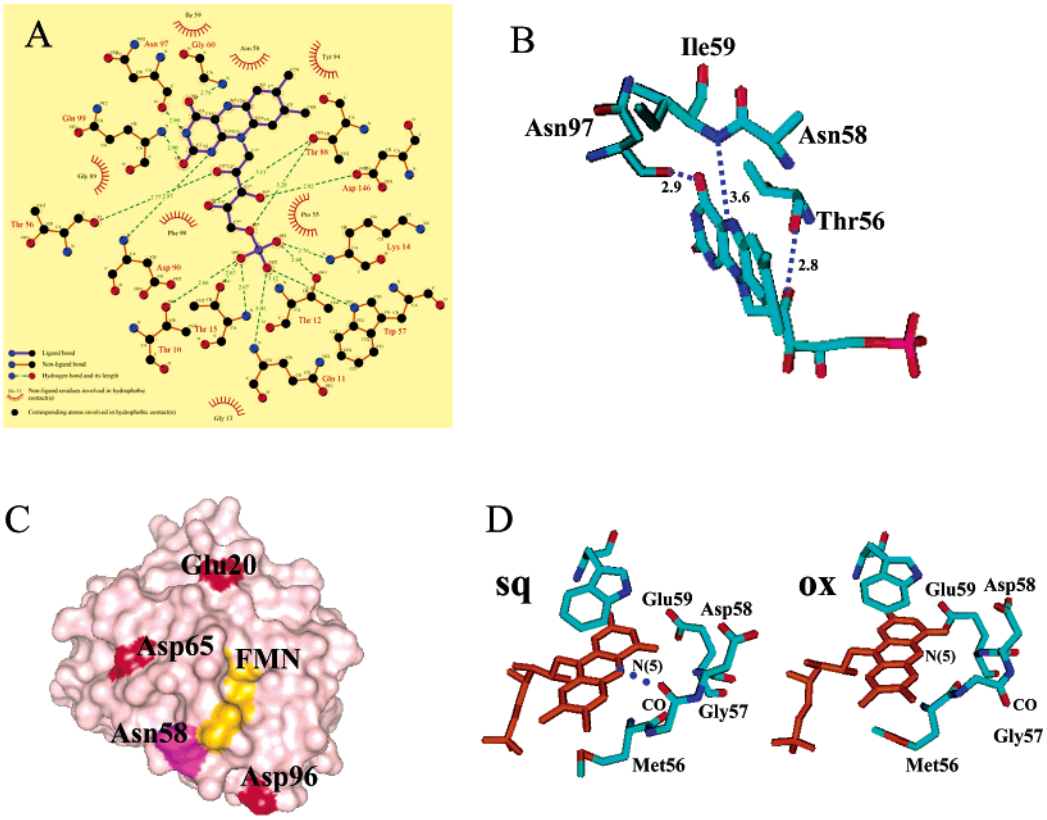

FIGURE 2: (A) FMN environment within *Anabaena* Fld. H bonds are denoted by dashed lines, and distances are in angstroms. The figure was produced with LIGPLOT (*56*). (B) Relative position of Thr56, Asn58, and Asn97 with regard to the FMN in *Anabaena* Fld. H bonds are shown by blue lines. (C) Surface representation of *Anabaena* Fld showing the localization of the negatively charged residues (in red) Glu20, Asp65, and Asp96 and the neutral residue Asn58 (in magenta). The FMN surface is shown in yellow. B and C were produced using PyMOL (*57*). (D) Representation of the *C. beijerinckii* Fld isoalloxazine environment in the semiquinone and oxidized states.

In some Flds, such as that from *Anabaena*, the isoalloxazine ring is stacked between a Tyr and a Trp (*19*, *21*, *22*, *27*, *31*−*33*). In these structures, the Tyr residue is positioned in a nearly coplanar orientation with the outer face of the isoalloxazine ring, whereas the Trp forms a large portion of the inner surface of the flavin-binding pocket. Three segments of ApoFld contribute to FMN binding: the phosphate-binding loop (residues 10−15 in *Anabaena* Fld) and the loops connecting β3 and α3 (residues 56−62) and β4 and α4 (residues 90−99) (Figures 1 and 2A) (*29*). In particular, the 56−62 and 90−99 segments contain residues in close contact with the isoalloxazine ring system (parts A and B of Figure 2) and are likely to influence the binding of FMN and the redox properties of the flavin (*4*, *16*, *17*, *34*).

Parts A and B of Figure 2 summarize the interactions, either hydrophobic or H bonds, that might contribute to FMN stabilization in oxidized *Anabaena* Fld. The Asp90 NH forms a bifurcated H bond with N(1) and O(2) of the flavin; the Gln99 backbone NH makes a H bond to O(2); the Asn97 main-chain CO is H-bonded to N(3); the Gly60 NH H-bonds to O(4); and the Thr56 CO H-bonds to N(1) of the flavin. The protein group closest to the key N(5) position of FMN is the Ile59 NH (Figure 2B). The distance between these two nitrogen atoms is 3.6 Å and therefore larger than usual for an H bond. However, the groups are well-oriented, suggesting that a weak H bond may be established (*21*). In addition to these H-bonding interactions, the isoalloxazine moiety makes nonpolar contacts with atoms from Asn58, Ile59, Gly60, Tyr94, and Asn97 (Figure 2A).

While the H-bond network observed in *Anabaena* Fld is essentially conserved in Fld structures from different species (*26*), the 56−62 segments vary considerably in both sequence and conformation. Additionally, conformational changes upon FMN reduction have been reported in this region. Thus, the analysis of the oxidized and semiquinone structures of *Anacystis nidulans*, *Clostridium beijerinckii*, and *Desulfovibrio vulgaris* Flds indicates that semiquinone formation is accompanied by a backbone rearrangement that allows a main-chain carbonyl O to form a H bond with the N(5)H present in the neutral flavin semiquinone (*15*, *23*, *24*). In *C. beijerinckii*, *D. vulgaris*, and *D. desulfuricans* Flds, this carbonyl O is contributed by a Gly, whereas in *A. nidulans* Fld it comes from an Asn (corresponding to Asn58 in *Anabaena* Fld) (*7*, *15*, *26*). Moreover, the formation of this

H bond is accompanied in some Flds by the breakage of a weak H bond to FMN N(5) that appears in oxidized Fld [with Val59 NH in *A. nidulans*, equivalent to Ile59 NH in *Anabaena* or with the side chain of Thr58 in *Chondrus crispus* Fld (*35*)]. Such backbone rearrangements appear to provide a versatile device for reduction potential modulation. The fact that the semiquinone states of *A. nidulans* and *Anabaena* Flds are less stable than those of Flds from other species has been related to the weaker H bond that is formed between the N(5)H of the flavin and the backbone CO of Asn compared to the bond formed with the smaller Gly (*7*). The three-dimensional structure of the *Anabaena* Fld semiquinone is not known, and it therefore remains to be confirmed whether a similar conformational change occurs in this protein.

In an attempt to further elucidate the roles played by the residues in the 56−62 and 90−99 segments in *Anabaena* Fld, we have introduced different mutations at key residues around the isoalloxazine moiety so that the polarity and/or the H-bond network is modified. The influence of the Thr56Gly, Thr56Ser, Asn58Cys, Asn58Lys, and Asn97Lys mutations on the reduction potentials and binding affinities of FMN in its three redox states has been determined. In addition, we have studied the effects of mutating three negatively charged residues on the surface of the protein that are close to the FMN but have no direct contact with the flavin ring (mutants Glu20Lys, Asp65Lys, and Asp96Asn; Figure 2C).

MATERIALS AND METHODS

Biological Material. Site-directed mutagenesis to produce the Asp96Asn mutant of *Anabaena* sp. PCC7119 Fld has been previously described (*36*). The Glu20Lys, Thr56Gly, Thr56Ser, Asn58Lys, Asn58Cys, Asp65Lys, and Asn97Lys mutants were produced using the QuickChange mutagenesis kit (Stratagene) and the following synthetic oligonucleotides (base changes are in bold): 5'-CTGAATCAGTAGC**GA**-AAATCATTCGAGACGAGTTTGG-3′ for Glu20Lys, 5'-GATTATTGGCTGTCCT**GG**TTGGAATATTGGC-3′ for Thr56Gly, 5'-GATTATTGGCTGTCCTA**GC**TGGAATAT-TGGC-3′ for Thr56Ser, 5'-CGCTTTGCAGTTCGCCAAT-**T**TTCCAAGTAGGACAGCC-3′ for Asn58Lys, 5′-GTTC-GCCAATA**CA**CCAAGTAGGA- 3′ for Asn58Cys, 5'-GGC-GAACTGCAAAGC**A**A**A**TGGGAAGGACTCTATTCAG-3′ for Asp65Lys, and 5'-CCAAATAGGTTACGCAGATAA-**A**TTTCAGGATGCGATCGG-3′ for Asn97Lys.

Mutations were verified by DNA sequence analysis. The expression and purification of the Fld mutants was essentially as described previously (*11*, *30*). The UV−visible absorption spectrum and SDS−PAGE patterns were used as purity criteria. ApoFld was obtained by treating the Fld with trichloroacetic acid at 4 °C in the presence of dithiothreithol. The precipitate of ApoFld was separated from FMN by centrifugation (*37*).

Spectroscopic Analysis. UV−vis spectra of Flds were recorded on a Kontron Uvikon 942 or a CARY 1 spectrophotometer. Extinction coefficients of the different Fld mutants in the fully oxidized state were determined in 50 mM Tris-HCl at pH 8.0 as described by Mayhew and Massey (*38*) using, for released FMN, a corrected extinction coefficient of 12.02 mM^{-1} cm^{-1} at 445 nm (*11*). Extinction coefficients for the neutral semiquinone state at 580 nm were determined from data obtained during anaerobic photoreduction in the presence of 5-deazariboflavin (dRf) and EDTA (see below). The maximum semiquinone state stabilized for each Fld form was determined as the intercept of the two linear sections of a plot of the absorbance at 580 nm versus the absorbance at 460 nm. Fluorescence spectra were recorded at 25 °C in a Kontron SFM25 spectrofluorimeter in 50 mM Tris-HCl at pH 8.0. Circular dichroism spectra were recorded at 25 °C in a Jasco 710 spectropolarimeter in a 1 cm path-length cuvette in 1 mM Tris-HCl at pH 8.0 and 25 °C. The protein concentrations were 0.7 μM for the far-UV and 4 μM for the near UV−vis regions of the spectrum. Photoreduction of protein-bound flavin was carried out at 25 °C in an anaerobic cuvette containing 15−25 μM Fld in the desired buffer, which also contained 1 mM EDTA and 2 μM dRf to initiate reduction via the highly reductive dRfH•radical. Reaction solutions were made anaerobic by several cycles of evacuation and flushing with O_2-free Ar. Absorption spectra were recorded after successive periods of irradiation with a 150 W light source and were used to calculate the concentration of the different redox states of the protein−flavin complex throughout the reduction process.

To carry out electron paramagnetic resonance (EPR) and electron spin−echo envelope modulation (ESEEM) spectroscopic measurements the Fld mutants were reduced anaerobically to the semiquinone state at 4 °C by light irradiation with a 150 W light source in the presence of 20 mM EDTA and 2.5 μM dRf in 10 mM HEPES at pH 7.0, as described previously (*39*, *40*). A Bruker ESP380E spectrometer operating in X band (9−10 GHz) was used for continuous wave (cw)-EPR and pulsed-EPR measurements. Spectra were taken at 15 K. The field position, at the center of the EPR signal, was selected to give a maximum echo intensity (*40*). The microwave pulse sequence was ($\pi/2 - \tau - \pi/2 - t_1 - \pi - t_2 - \pi/2$) for the 4-pulse 2D-ESEEM (HYSCORE) experiment. Appropriate phase cycling was applied to remove unwanted echoes. 1D- and 2D-ESEEM experiments were recorded as indicated elsewhere (*40*).

Reduction Potential Determinations. Midpoint reduction potentials of Glu20Lys, Thr56Gly, Thr56Ser, Asn58Cys, Asn58Lys, Asp65Lys, Asp96Asn, and Asn97Lys Flds were determined by anaerobic photoreduction in the presence of 1 μM dRf and 20 mM EDTA at 25 °C using a saturated calomel electrode as the reference (*41*). Stepwise Fld photoreduction was achieved by irradiating the solution (with the cell immersed in ice water) with light from a 250 W slide projector for periods of approximately 1 min. After reduction, the cell was placed in a temperature-controlled holder in a Cary 1 spectrophotometer. The solution potential was monitored using a Sycopel Ministat potentiostat. Equilibration of the system was considered established when the measured potential remained stable for 10 min, and the UV−vis spectrum was then recorded. The concentrations of the different redox species in equilibrium were determined from the absorbance spectra. The two one-electron steps in reduction could be analyzed separately because only oxidized and semiquinone states were present during most of the first step and only semiquinone and hydroquinone Flds were present during most of the second one. The concentration of semiquinone was calculated from the absorbance of the

Table 1: UV−Visible Spectral Properties of WT and Mutated Flavodoxins in the Oxidized and Semiquinone States[a]

Fld form	oxidized λ_{max} (nm) I	oxidized λ_{max} (nm) II	oxidized ε_{max} (mM^{-1} cm^{-1}) I	oxidized ε_{max} (mM^{-1} cm^{-1}) II	$\varepsilon_I/\varepsilon_{II}$	isosbestic points ox/sq (nm)	semiquinone λ_{max} (nm)	semiquinone ε_{max} (M^{-1} cm^{-1})
WT	463	374	9.4	8.6	1.1	516.3	578	5.0
T56G	465	373	9.4	8.0	1.2	528.3	581	3.5
T56S	464	372	8.7	7.6	1.1	520.3	580	4.6
N58C	464	370	8.6	8.6	1.0	518.3	574	4.4
N58K	463	370	8.2	7.6	1.1	524.3	580	3.5
N97K	463	372	9.1	7.6	1.2	516.3	574	4.6

[a] Data obtained in 50 mM Tris-HCl at pH 8.0 and 25 °C.

580 nm band (maximum and extinction coefficient used for each Fld form can be found in Table 1), and the concentration of the other species was determined by subtraction of the semiquinone concentration from the total concentration of Fld. The midpoint potentials for the redox couples were calculated by linear regression analysis of the plots of potential versus logarithm of the concentration ratio (oxidized/semiquinone or semiquinone/hydroquinone) according to the Nernst equation

$$E = E_m + (0.059/n)\log([ox]/[rd]) \quad (1)$$

Data points in the region of maximal semiquinone accumulation were not included in the regression because, in this region, all three redox species could be present. The midpoint potentials are reported relative to the potential of the standard hydrogen electrode. Typical experimental solutions contained 25−40 μM protein, 1−3 μM mediator dyes, 2 μM dRf, and 1 mM EDTA at 25 °C. The following dyes were used as mediators: 1 μM anthraquinone-2,6-disulfonate (−184 mV) and 1 μM anthraquinone-2-sulfonate (−225 mV) for the determination of $E_{ox/sq}$ and 1 μM benzyl viologen (−359 mV) and 1 μM methyl viologen (−446 mV) for the determination of $E_{sq/rd}$. When required, protein spectra were corrected for the spectra of oxidized or reduced mediators. The buffer used for the determination of the reduction potential at pH 8.0, 7.3, and 7.0 was 50 mM Tris-HCl, whereas determinations at pH 6.6, 5.9, and 5.7 were carried out in 20 mM potassium phosphate. The error in the $E_{ox/sq}$ and $E_{sq/rd}$ determined was estimated to be ±3 mV.

Dissociation Constants. The dissociation constants of the ApoFld:FMN_{ox} complexes were determined fluorometrically in a SMF25 spectrofluorimeter at 25 °C in the dark. Excitation was at 445 nm, and emission was recorded at 525 nm. The FMN used was >95% pure according to reverse-phase HPLC. In a typical experiment, 1 mL of 200 nM FMN in 50 mM Tris-HCl at pH 8.0 was titrated with aliquots of 10−100 μM ApoFld solutions. Binding of the protein to the cofactor strongly quenches its fluorescence emission. After each protein addition, the system was allowed to reach equilibrium for 2 min. The dissociation constants were calculated by fitting the fluorescence emission to the following equation (*28*):

$$F = F_{final} + F_\delta(dC_F - [(C_A + K_d + dC_F) - [(C_A + K_d + dC_F)^2 - 4C_A dC_F]^{1/2}]/2 \quad (2)$$

where F is the observed fluorescence emission intensity after each addition, F_{final} is the remaining emission intensity at the end of the titration, F_δ is the difference in emission intensity between 1 μM free FMN and 1 μM Fld, C_A is the total protein concentration after each addition, C_F is the starting concentration of FMN, and d is the dilution factor of this initial concentration (initial volume/total volume) after each addition. Error in the determination of K_d values was estimated to be ±10%.

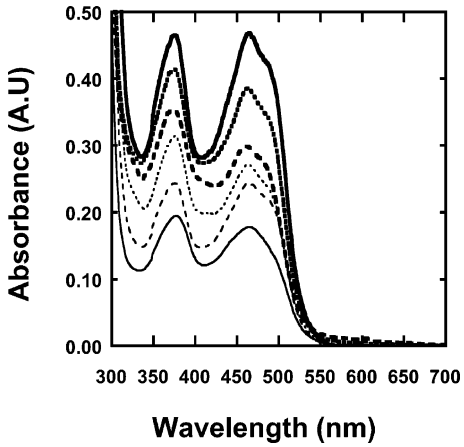

FIGURE 3: Absorption spectra of WT (bold line), Thr56Gly (thin line), Thr56Ser (broken thin line), Asn58Cys (dotted thin line), Asn58Lys (broken bold line), and Asn97Lys (dotted bold line) *Anabaena* Fld forms in the visible region. The spectra were recorded in 50 mM Tris-HCl at pH 8.0 and room temperature. Different protein concentrations were used to clarify the figure.

Measurement of the Cavity Volume. On the basis of the *Anabaena* Fld three-dimensional structure (PDB accession code 1flv), models for the different mutants studied have been generated using the Swiss-PdbViewer by using the replace routine (GlaxoSmithKline R&D). The cavity volume was calculated for each all-atom Fld mutant model with a probe radius of 1.4 Å using the method implemented in the Swiss-PdbViewer (*42*).

RESULTS

Expression, Purification, and Spectral Properties of the Different Fld Mutants. The levels of expression of Glu20, Thr56, Asn58, Asp65, Asp96, and Asn97 mutants and their spectral properties were similar to those of the wild-type (WT) Fld (not shown), indicating that no major structural perturbations had occurred. The Thr56Gly mutant lost a fraction of its FMN during purification, an early indication that the flavin in this protein is bound rather weakly.

Although the absorption spectra of the mutants are similar to that of WT Fld, differences occur in the shapes of the spectra and also in the extinction coefficients at the maxima (Figure 3 and Table 1). In most cases, the extinction coefficients at the maxima around 460 nm are smaller than that of the WT, and the spectra of Asn58Lys and especially that of Thr56Gly show an important decrease of the characteristic shoulder found at 480 nm in WT Fld, indicating that the flavin environment has been modified. Photoreduction under anoxic conditions showed that all of the mutants stabilize the blue neutral semiquinone. However, the absorption spectra of the semiquinone forms of the mutants differ from that of the WT, both in the position of the maximum around 580 nm and in the extinction coefficient at the maximum. An isosbestic point between the spectra of the

Table 2: Midpoint Reduction Potentials and Percentage of Maximal Semiquinone Stabilized for the Different Fld Forms[a]

Fld form	$E_{ox/sq}$	$E_{sq/rd}$	% sq	Fld form	$E_{ox/sq}$	$E_{sq/rd}$	% sq
WT	−266	−439	97	N58K	−289	−407	72
E20K	−265	−430	94	D65K	−247	−423	90
T56G	−264	−376	75	D96N	−279	−426	88
T56S	−251	−445	93	N97K	−282	−421	86
N58C	−272	−450	90	FMN free[b]	−269	−215	14

[a] Data obtained in 50 mM Tris-HCl at pH 8.0 and 25 °C. [b] Data from refs *54* and *55*.

oxidized and semiquinone forms of WT Fld occurs at 516.3 nm; the corresponding isosbestic point for most of the mutants is different (Table 1). The extent of semiquinone stabilization at half-reduction is less for the mutants than for WT Fld, and the decrease is especially marked for Thr56Gly and Asn58Lys (Table 2, values determined from the reduction potentials).

The fluorescence emission of FMN bound to WT Fld is very low (less than 5% of free FMN under our experimental conditions) as a result of the strong quenching by the apoprotein (*11*). The flavin fluorescence of the mutants is similar to that of the WT, except in the case of Thr56Gly and Asn58Lys, which display 29 and 9%, respectively, of the fluorescence of free FMN. The greater fluorescence of these two mutants suggests that the FMN in them has more exposure to the external medium. The circular dichroism UV spectra of mutated Fld forms are very similar to that of the WT, again indicating that the global protein fold is not affected by the introduced mutations.

The semiquinone forms of all of the Fld mutants that were investigated gave the isotropic cw-EPR spectrum, centered at $g = 2.005$, that was described for WT Fld semiquinone (*39*). Similarly, the 1D- and 2D-ESEEM spectra of the different Fld semiquinone mutants are very similar to those of the WT (*40*) (not shown). No significant differences could be discerned between the different Fld mutants and the WT protein either in the ^{14}N hyperfine couplings of the flavin ring nitrogens, in 1D or 2D experiments, or in the calculated isotropic and anisotropic hyperfine coupling constants for H(5). This indicates that the individual residues modified around the flavin ring do not influence the electron density distribution in the semiquinone form of the FMN.

Reduction Potentials. The average slopes of the Nernst plots for WT Fld and its mutants were 59.8 ± 2.0 and 60.8 ± 3.0 mV for $E_{ox/sq}$ and $E_{sq/rd}$, respectively (Figure 4). The midpoint reduction potentials calculated from the Nernst plots for the WT protein at pH 8.0 are similar to those reported earlier (*43*). In general, although both midpoint reduction potentials, $E_{sq/rd}$ and $E_{ox/sq}$, change for the mutants, larger effects are seen in $E_{sq/rd}$ (ΔE from −11 to +63 mV) than in $E_{ox/sq}$ (ΔE from −23 to +19 mV). The effects are greatest for the Thr56Gly and Asn58Lys mutants. Thus, replacement of Thr56 by the smaller residue Gly makes $E_{sq/rd}$ less negative ($\Delta E = +63$ mV), while the mutation has no effect on $E_{ox/sq}$. The potentials for the two steps tend to converge so that the semiquinone that is stabilized at half-reduction decreases from 97% for WT Fld to only 75% for the mutant (Table 2). It is notable that, when Thr56 is replaced by Ser, a side chain that is also able to form a H bond, only small changes in $E_{sq/rd}$ and $E_{ox/sq}$ occur (Table 2). In contrast, when Asn58

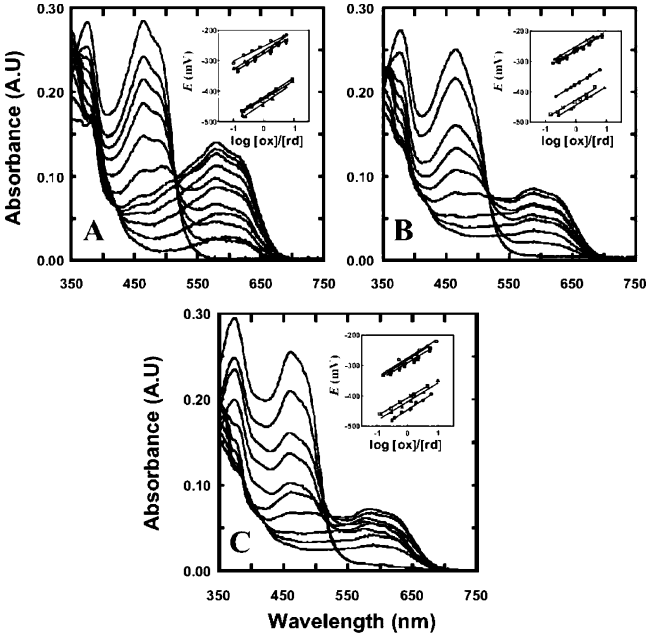

FIGURE 4: UV−visible spectra obtained during photoreduction and redox titration of (A) WT, (B) Thr56Gly, and (C) Asn58Lys Fld forms. The insets show the Nernst plots for the different Fld forms: (A) oxidized/semiquinone of WT (△), Asp65Lys (○), and Asp96Asn (■) and semiquinone/hydroquinone of WT (▲), Asp65Lys (●), and Asp96Asn (□); (B) oxidized/semiquinone of Glu20Lys (■), Thr56Gly (○), and Thr56Ser (△) and semiquinone/hydroquinone of Glu20Lys (□), Thr56Gly (●), and Thr56Ser (▲); (C) oxidized/semiquinone of Asn58Cys (○), Asn58Lys (■), and Asn97Lys (△) and semiquinone/hydroquinone Asn58Cys (●), Asn58Lys (□), and Asn97Lys (▲).

is replaced by the charged residue Lys, both $E_{sq/rd}$ and $E_{ox/sq}$ change, causing $E_{ox/sq}$ to become more negative ($\Delta E = -23$ mV) and $E_{sq/rd}$ to become less negative ($\Delta E = +32$ mV). Again, the decrease by 55 mV in the difference in reduction potential between the two steps of reduction is consistent with the decrease observed in the maximum semiquinone stabilized by this mutant (25% less than for WT Fld) (Table 2). However, when Asn58 is replaced by Cys, the changes are smaller, with both potentials becoming slightly more negative, $\Delta E_{sq/rd} = -11$ mV and $\Delta E_{ox/sq} = -6$ mV. Changes also occur in the $E_{ox/sq}$ and $E_{sq/rd}$ values of the Asp65Lys, Asp96Asn, and Asn97Lys mutants (Table 2). In contrast, when the surface charge from the side chain of Glu20 is reversed in the Glu20Lys mutant, neither reduction potential is affected.

The effects of pH on the reduction potentials were determined for WT Fld and for the Thr56Gly and Asn58Lys mutants in the pH range from 6 to 8 (Figure 5). Data obtained for WT Fld confirmed an earlier study (*43*), which showed that $E_{ox/sq}$ is pH-dependent with a slope of −51 mV/pH unit and that $E_{sq/rd}$ is pH-independent at high pH but becomes pH-dependent as the pH is decreased below about pH 7 (Figure 5). The slope for $E_{ox/sq}$ is smaller than might be expected for the addition of one electron and a proton to form the neutral semiquinone (theoretical value −59 mV at 25 °C), possibly reflecting ionizable groups on the apoprotein that might alter the FMN environment and modulate the reduction properties of the flavin−protein complex. The slope change for $E_{sq/rd}$ has been ascribed to a redox-linked protonation of the hydroquinone complex with an apparent pK_a of 6.1 (*43*). Similar pH-dependent changes in $E_{sq/rd}$ have

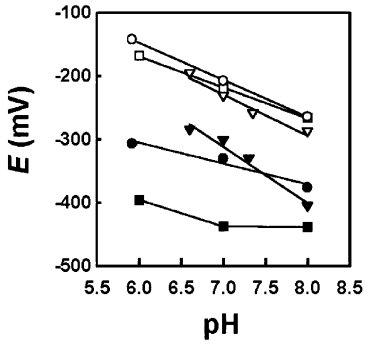

FIGURE 5: pH dependence of the $E_{ox/sq}$ values of WT (□), Thr56Gly (○), and Asn58Lys (▽) Flds and of $E_{sq/rd}$ values of WT (■), Thr56Gly (●), and Asn58Lys (▼) Flds.

Table 3: Dissociation Constants for the ApoFld:FMN_{ox} Complexes and Free Energies for the Formation of the Corresponding Oxidized, Semiquinone, and Hydroquinone Complexes[a]

Fld form	K_d (nM)[b]	ΔG_{ox} (kcal mol^{-1})[c]	ΔG_{sq} (kcal mol^{-1})[d]	ΔG_{rd} (kcal mol^{-1})[d]
WT	3.0	−11.69	−11.76	−6.61
E20K	4.7	−11.42	−11.52	−6.57
T56G	554	−8.60	−8.71	−5.01
T56S	9.6	−11.00	−11.41	−6.12
N58C	50	−10.02	−9.95	−4.54
N58K	15.7	−10.71	−10.25	−5.83
D65K	6.0	−11.28	−11.78	−7.00
D96N	2.5	−11.80	−11.57	−6.72
N97K	18.6	−10.60	−10.31	−5.57

[a] Data obtained in 50 mM Tris-HCl at pH 8.0 and 25 °C. [b] Determined from fluorometric titrations of FMN_{ox} with WT or mutated ApoFlds. [c] Calculated from data in b. [d] Calculated from data in c using eqs 3 and 4.

been reported for other Flds. There is evidence that the pK_a is not associated with the flavin itself but rather with ionization of group(s) on the apoprotein (*44*, *45*).

The pH dependencies of $E_{ox/sq}$ for the Thr56Gly and Asn58Lys Fld mutants are close to the theoretical value (slopes of −61 and −65 mV/pH were found for Thr56Gly and Ans58Lys, respectively). The pH dependencies of $E_{sq/rd}$ for these two mutants are even more different from that of the WT protein, with the values for both mutants changing throughout the pH range investigated (Figure 5). In addition, the slope for the Thr56Gly mutant is only −33 mV/pH, while that for Asn58Lys is larger (−89 mV/pH). These different pH effects mean that while at pH values below 7 the redox potential for the semiquinone/hydroquinone couple is much less negative than that of the WT (at least +130 mV for the Asn58Lys mutant), with the differences becoming smaller at high pH (only +32 mV for Asn58Lys at pH 8).

Dissociation Constants. Dissociation constants (K_d) for the ApoFld:FMN_{ox} complexes have been determined for WT *Anabaena* Fld and for the mutants (Table 3). The value determined for the WT complex (3 nM in 50 mM Tris-HCl at pH 8.0) is about 10 times larger than previously reported (0.26 nM in 50 mM Mops at pH 7.0) (*28*). The difference can be attributed to the different experimental conditions used in the two measurements, because the K_d for a variety of Flds is known to be affected by the type of buffer, by the ionic strength, and especially, by the pH that in this case suffers a change of 1 unit (*28*, *46*−*48*). The K_d values for the Glu20Lys, Asp65Lys, and Asp96Asn mutants of *Anabaena* Fld are similar to that of WT Fld under the same

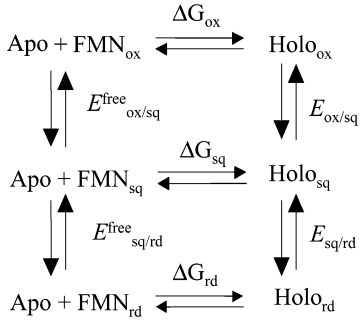

FIGURE 6: Thermodynamic cycle showing the relationship between the reduction potentials of free and bound FMN with the affinity constants of the oxidized, semiquinone, and hydroquinone ApoFld:FMN complexes (*11*).

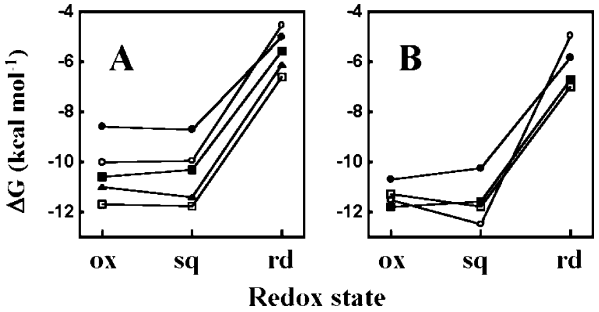

FIGURE 7: Binding energy profiles versus reduction for WT and mutated ApoFld:FMN complexes. (A) WT (□), Thr56Gly (●), Thr56Ser (▲), Asn58Cys (○), and Asn97Lys (■); (B) Glu20Lys (○), Asp96Asn (■), Asn58Lys (●), and Asp65Lys (□).

experimental conditions, while the remaining mutants bind oxidized FMN less strongly (Table 3). The K_d values for the Thr56Ser, Asn58Lys, and Asn97Lys mutants are increased by 3.2, 5.2, and 6.2-fold, respectively, compared with that of the WT protein. Finally, the K_d for the Asn58Cys mutant shows a 17-fold increase, while the Thr56Gly mutant shows the weakest affinity (K_d increased 184-fold).

The reduction potentials of ApoFld:FMN complexes are linked to the binding affinities of the different FMN redox forms by the thermodynamic cycle shown in Figure 6, allowing the K_d values for the corresponding semiquinone and hydroquinone complexes to be calculated (*11*). Thus, the free energy for the ApoFld:FMN_{ox} (ΔG_{ox}) complex can be obtained directly from the K_d values, while those of the ApoFld:FMN_{sq} (ΔG_{sq}) and ApoFld:FMN_{rd} (ΔG_{rd}) complexes can be calculated from the following equations (*11*):

$$\Delta G_{sq} = \Delta G_{ox} - F(E_{ox/sq} - E_{ox/sq}^{free}) \quad (3)$$

$$\Delta G_{rd} = \Delta G_{ox} - F(E_{ox/sq} + E_{sq/rd} - E_{ox/sq}^{free} - E_{sq/rd}^{free}) \quad (4)$$

where F is Faraday's constant.

The data obtained (Table 3) show that the stability of the semiquinone complex in WT Fld is similar to that of the oxidized complex, while further reduction of the FMN destabilizes the flavin−protein interaction (Figure 7). The corresponding energy profiles of the Fld mutants along the reduction are similar to that of the WT, with the oxidized and semiquinone complexes having similar strength and the interactions with the hydroquinone flavin being significantly weaker. However, the ΔG values vary in the different mutants. Thus, the ΔG_{ox}, ΔG_{sq}, and ΔG_{rd} values for the

ApoFld:FMN interactions of the Glu20Lys, Thr56Ser, Asp65Lys, and Asp96Asn mutants are similar to those of WT Fld (Table 3 and Figure 7). When Thr56 is replaced by Ser, a slight weakening of the oxidized and hydroquinone complexes occurs, whereas the affinity of the protein for the FMN semiquinone is unaffected. In contrast, the changes associated with the other mutants are larger. Thus, the substitution of Asn58 or Asn97 by residues with a positively charged side chain clearly displaces the free energy profile to less negative values (Figure 7). For Asn58Lys, the destabilization of the semiquinone and hydroquinone complexes is larger than that of the oxidized complex, whereas the greater destabilization for the Asn97Lys mutant occurs with the hydroquinone complex. Moreover, when Asn58 is replaced by a Cys, further destabilization of the interaction in all redox states is observed, again with the greatest effect on the hydroquinone complex. Finally, the largest overall effect is observed when Thr56 is replaced by Gly. Complexes of this mutant with FMN in all redox states are much weaker than in the WT protein, and the effects are greatest for the oxidized and semiquinone complexes.

DISCUSSION

The factors involved in modulation of reduction potentials in flavoproteins have been an object of study for many years, and the molecular basis for differences in redox potentials is still a matter of extensive discussion. Mutations have been introduced in the close environment of the flavin in *Anabaena* Fld to modify not only the electrostatic environment of the isoalloxazine ring but also the solvent accessibility of the flavin, as indicated by the differences found between the UV−vis absorbance and FMN fluorescence quenching properties of the different mutants (Table 1). The data indicate that, when the electrostatic properties of amino acid side chains within a radius of 14 Å of the isoalloxazine system are modified, substantial changes occur in both reduction potentials, $E_{ox/sq}$ and $E_{sq/rd}$ (Table 2). However, only small effects occur when Glu20, a negatively charged amino acid on the surface of Fld and more than 20 Å from the isoalloxazine moiety, is replaced by Lys. Additionally, for the Thr56Gly mutant, only $E_{sq/rd}$ is modified (Table 2).

Modulation of the sq/rd Potential by the Protein Environment. Structural and functional studies have established that electrostatic interactions are a determinant factor in the sq/rd equilibrium in Flds. Because the hydroquinone form of FMN in Fld is normally not protonated at N(1) (*49*) and because this position is in an environment of negative charge in the protein, repulsive forces are generated (*4*, *50*). A careful analysis of the $E_{sq/rd}$ values for the different *Anabaena* Fld mutants indicates that either removal of negatively charged side chains or introduction of positive ones shifts $E_{sq/rd}$ to less negative values, with the magnitude of the change depending on the distance and on the relative location of the modified charge relative to the isoalloxazine ring. Thus, neutralization of the Asp96 side-chain charge, situated on the Fld surface 10 Å away from the flavin ring, by an Asn, produces a change of +13 mV in $E_{sq/rd}$, whereas introduction of Lys in the direct environment of the FMN isoalloxazine ring at positions 58 or 97 (side chains around 4 and 5 Å away from the ring, respectively) causes displacement of $E_{sq/rd}$ to less negative values by +32 and +18 mV, respectively. Moreover, the $E_{sq/rd}$ also shifts moderately to less negative values upon charge reversion of Glu20 (by +9 mV) and Asp65 (by +16 mV), residues situated on the Fld surface further away from the flavin ring by 20 and 13 Å, respectively. These observation might indicate that the positive charges introduced in the flavin environment partially neutralize the negative charge that interacts with the negative charge at N(1) of the FMN hydroquinone. Similarly, $E_{sq/rd}$ also becomes less negative when Lys replaces either Asn58 or Asn97. The results clearly show that elimination of negative charges in the FMN surroundings favors reduction to the hydroquinone, an effect that is also produced by partially balancing the negative charge with the positive charge. Our observations are in agreement with earlier ones that indicate that the generally negative electrostatic environment generated by negatively charged residues in the FMN surroundings contributes to the negative $E_{sq/rd}$ value in Flds (*4*, *8*, *9*, *51*). Theoretical calculations on the Fld system estimate a contribution of −4 mV (at an ionic strength of 100 mM) per negatively charged residue to the shift of the free FMN potential (*52*), and experimental neutralization of negatively charged residues in *D. vulgaris* Fld has shown an increase of +15 mV in the $E_{sq/rd}$ value per mutated residue (*4*, *10*). A comparison of the crystal structures of the Asp95Asn mutant in its three redox states with the corresponding structures of the WT of this protein revealed that the conformations of the two protein loops that bind the flavin hydroquinone are different in the mutant and that the phenol ring of Tyr98 rotates so that it makes an edge−face interaction with the isoalloxazine rather than a face−face interaction (*9*). Similarly large structural changes occur in the oxidized forms of several Gly61 mutants of this Fld (*17*), emphasising that mutations at the flavin site can have profound structural consequences. The importance of electrostatic repulsion in the control of the sq/rd potentials in Flds has also been demonstrated with the proteins of *C. beijerinckii*, *A. nidulans*, and *M. elsdenii* (*7*, *8*, *50*).

Solvent accessibility is another important factor that has been shown to contribute to modulating $E_{sq/rd}$. Thus, replacement of the aromatic side chain that stacks against the flavin ring by a smaller amino acid leads to a displacement of $E_{sq/rd}$ to less negative values (*3*, *11*). In addition, the more negative values for *A. nidulans* and *D. vulgaris* Flds compared with that for the *C. beijerinckii* protein can be explained by a channel for the solvent at the pyrimidine end of the isoalloxazine ring in the *C. beijerinckii* Fld that is blocked by three to five additional residues in the other two proteins (*7*). Among the mutations analyzed in the present study, we can also observe how the accessibility of the flavin to the solvent influences $E_{sq/rd}$. Thus, when Thr56 is replaced by Gly, a +63 mV increase of $E_{sq/rd}$ is observed, whereas replacement by a more bulky residue such as Ser produces a value for this parameter that is similar to that of WT Fld. The theoretical calculation indicates that the volume of the internal cavities increases only in the case of the Thr56Gly mutant. In addition, the changes are only observed in the close environment of the FMN and the mutated side chain, where a 20 $Å^3$ cavity is present in WT Fld. In the case of the Thr56Gly mutant, the cavity is enlarged to 44 $Å^3$ and a second smaller cavity (16 $Å^3$) appears next to it (Figure 8A).

Modulation of the ox/sq Potential by the Protein Environment. Transition from the oxidized to the semiquinone state

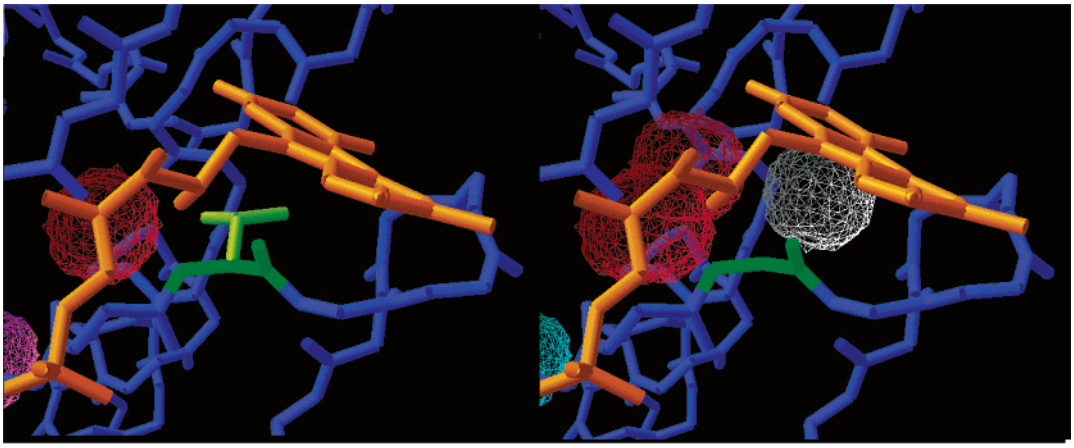

FIGURE 8: Representation of the cavities formed around the isoalloxazine system in WT and Thr56Gly Flds. The *in silico* Thr56Gly Fld mutation has been obtained using the Swiss-PdbViewer. The same program has also been used to add H atoms, minimize the structures, calculate the cavity volumes, and produce the figure. The protein backbone is represented in dark blue; FMN, in orange; and position 56, in green. One cavity is found in the close environment of WT Fld isoalloxazine (red). This cavity is enlarged in the case of the mutant (also in red), where a new cavity is also formed (gray).

of *A. nidulans*, *C. beijerinckii*, and *D. vulgaris* Flds has been shown to be accompanied by a backbone peptide rearrangement (O-up conformation, Figure 2D). Thus, a comparison of these oxidized and semiquinone 3D structures indicates that, upon reduction to the semiquinone state, formation of a new H bond occurs between a carbonyl O of the twisted backbone and the N(5)H position of the ring O58−N(5)H (*A. nidulans* numbering) (*7*) and that the NH59 to N(5) contact that is found in the oxidized state is lost. Therefore, this peptide rearrangement appears to provide a versatile device for manipulation of the ox/sq potential. Although the amide group of Ile59 in oxidized *Anabaena* Fld is known to establish a weak H bond with the N(5) of the flavin ring (*21*), the structure of the semiquinone of this Fld has not been determined and there are no data to confirm the existence of structural changes in the backbone upon reduction to the semiquinone Fld state. However, the structural similarities between *Anabaena* and *A. nidulans* Flds and the fact that the loop sequence Trp57-Asn58-Ile59-Gly60-Glu61 in *Anabaena* Fld is conserved in *A. nidulans* Fld with only Ile59 substituting for a Val, suggest that the Asn58−Ile59 region in *Anabaena* Fld would similarly experience rearrangement in the transition from the oxidized form to the semiquinone (Figure 1). Thus, previous studies have shown that replacement of Ile59 by a Lys in *Anabaena* Fld produces a displacement of $E_{ox/sq}$ to more negative values (*53*). This proposed that conformational change might act in two ways, first, by altering flavin−protein contacts and, second, by modifying the conformational stability of the protein itself. It has been demonstrated that replacement of the N(5)−HN59 interaction in the oxidized state by the N(5)H−O58 bond in the semiquinone state is energetically favorable because N(5)H−O58 is the strongest of the two H bonds (*7*). On the other hand, the conformation adopted by the Asn58 side chain in *A. nidulans* Fld has lower energy in the oxidized state than in the semiquinone state (*7*). However, this energy difference might be compensated by changes at Ile59. One key difference between *C. beijerinckii* Fld and the proteins from *A. nidulans* and *Anabaena* is the presence of Asn at position 58 in the last two proteins instead of Gly. This Asn residue raises the energy of the O-up semiquinone conformer (*7*), thus making reduction more difficult and producing a decrease in the ox/sq potential. In fact, the Asn58Gly substitution in *A. nidulans* Fld produces the expected increase in $E_{ox/sq}$ (*7*). In this context, replacement of Asn58 of *Anabaena* Fld by a Lys produces a more negative $E_{ox/sq}$ value (by −23 mV) compared to that of the WT. The effect might correspond to an increase in the conformational energy of the peptide Asn58-Ile59 in the semiquinone state of this mutant by comparison with that of WT Fld. However, changes in the interaction between residue Asn58 and N(5)H cannot be discounted as secondary contributors to the potential shifts. In fact, the *Anabaena* Fld structure shows that this mutation might break hydrophobic interactions between the side chain of Asn58 and C6, C7, and C(7)M atoms of FMN. Finally, the introduction of a positive-charged residue near the neutral semiquinone can cooperate in raising the energy for the conversion oxidized semiquinone.

Dependence of Reduction Potentials on pH. Although no major alterations are detected in the $E_{ox/sq}$ values of the mutants, changes in the slopes of $E_{ox/sq}$ versus pH for the mutants compared to that of WT Fld and of the theoretical value expected for the addition of one electron and one proton to give the neutral semiquinone suggest that the mutations introduced affect the redox-linked protonation of some ionizable group in the flavin environment that contributes to the modulation of the $E_{ox/sq}$ potential.

Because no structural changes accompany reduction of flavodoxins from the semiquinone to the hydroquinone, it has been difficult to establish the basis for their very low $E_{sq/rd}$ potentials. However, it is accepted that in the Fld-reduced state the FMN ring remains unprotonated (anionic) and that the change in slope of $E_{sq/rd}$ (with $pK_a \sim 6-7$) reflects a change in the protonation state of the apoprotein, either of a single nearby carboxylate side chain or to the combined effects of several negatively charged side chains around the flavin-binding site (*44*, *45*, *50*).

The introduction of a Gly at the position of Thr56 or of a Lys at Asn58 evidently increases the value of the apparent

pK_a of *Anabaena* Fld. Although our data are insufficient for the new values to be calculated, they appear to be greater than p$K_a = 8$. Moreover, because the amino acids that were introduced are completely different both in their physicochemical properties and in their locations relative to the FMN ring, the reasons for the changes are probably different for the two mutants and related to conformational changes in the flavin ring environment. Unfortunately, none of the mutant proteins has crystallized in a form suitable for structural determination by X-ray crystallography. However, our 3D models suggest that, when Thr56 is replaced by Gly, cavities are produced around the N(1) and N(3) atoms of the flavin ring (Figure 8). In solution, such cavities might either be filled by solvent molecules or by atoms of the proteins if small conformational changes are produced in the area. It seems likely that these structural changes account for the shifts of $E_{sq/rd}$ to more positive values, for the decreases in the slope for the $E_{sq/rd}$ pH dependence, and for the displacement of the apparent pK_a of the hydroquinone to larger values. The shifts of $E_{sq/rd}$ suggest that the unfavorable interactions between anionic semiquinone and the protein environment are decreased in the mutants, possibly by an increase in the dielectric constant of the N(1) environment caused by the entrance of solvent molecules.

Role of Fld Residues in the ApoFld:FMN Interaction. The most noticeable change in K_d for the complexes ApoFld:FMN is for the Thr56Gly mutant with a K_d 184-fold higher than for WT Fld that corresponds to a change in ΔG of 3 kcal mol^{-1}. Thr56 establishes different interactions with FMN. These include a H bond between the backbone O and O(2′) of FMN and hydrophobic interactions between the side-chain atoms and N(1), C(2), O(2), N(3), C(4), O(4), and C(4a) atoms of FMN. Furthermore, the OG1 atom is involved in a H-bond network in the neighborhood of the FMN, interacting with Asp100 and Ala101 (*21*). All of these interactions stabilize the ApoFld:FMN complex in its three redox states. The substitution of Gly for Thr breaks the interactions established by the Thr side-chain atoms, causing the ApoFld:FMN binding to be weaker. Furthermore, a Gly in this position makes FMN more accessible to the solvent. In the case of the Thr56Ser mutant, the H-bond network in the vicinity of the FMN does not change, and although some of the hydrophobic interactions with FMN atoms may disappear as a consequence of the longer distance between them and Ser56, the ApoFld:FMN binding is not affected to a great extent. The O atom of Asn97 of *Anabaena* Fld forms an H bond with N(3) of FMN, and Asn97 is also involved in the H-bond network surrounding the FMN. It forms four H bonds, two with Asp100, one with Tyr94, and another with Gln99. Assuming that no structural changes occur that affect position 97, at least one H bond must be broken by the introduction of a Lys, the one with Asp100. Moreover, hydrophobic interactions with C(4) and O(4) of FMN should also be broken. All of these considerations lead to an ApoFld that forms a slightly weaker complex with FMN.

All three redox states of FMN are bound more weakly by Asn58Lys Fld than by WT Fld. This weaker binding might be a consequence of the different structural arrangements of the peptide Asn58-Ile59 and/or a different pattern of ApoFld:FMN interactions in the oxidized, semiquinone, and hydroquinone states. In the oxidized state, the H bond between Ile59 and N(5)H can be weaker than in WT Fld, whereas in the complexes ApoFld:FMN_{sq} and ApoFld:FMN_{rd}, the H bond between Asn58 and N(5)H is the one that is affected.

In conclusion, the data presented here indicate that flavodoxin regulates the FMN redox properties by limiting the solvent accessibility to the isoalloxazine ring, by controlling the hydrophopicity and electrostatic properties of its environment. In direct relationship with such observations, our data support the idea that the pK_a values of protein ionizable groups and H-bond networks around the flavin ring are important determinants of the ApoFld:FMN interaction strength.

ACKNOWLEDGMENT

We thank Drs. P. J. Alonso and J. I. Martínez from the Departamento de Física de la Materia Condensada—I.C.M.A., Universidad de Zaragoza, for the recording and interpretation of the EPR and HYSCORE spectra.

REFERENCES

1. Mayhew, S. G., Foust, G. P., and Massey, V. (1969) Oxidation−reduction properties of flavodoxin from *Peptostreptococcus elsdenii*, *J. Biol. Chem. 244*, 803−810.
2. Ludwig, M. L., and Luschinsky, C. L. (1992) Structure and redox properties of Clostridial flavodoxin, in *Chemistry and Biochemistry of Flavoenzymes III* (Muller, F., Ed.) pp 427−466, CRC Press, Boca Raton, FL.
3. Swenson, R. P., and Krey, G. D. (1994) Site-directed mutagenesis of tyrosine-98 in the flavodoxin from *Desulfovibrio vulgaris* (Hildenborough): Regulation of oxidation−reduction properties of the bound FMN cofactor by aromatic, solvent and electrostatic interactions, *Biochemistry 33*, 8505−8514.
4. Zhou, Z., and Swenson, R. P. (1995) Electrostatic effects of surface acidic amino acid residues on the oxidation−reduction potentials of the flavodoxin from *Desulfovibrio vulgaris* (Hildenborough), *Biochemistry 34*, 3183−3192.
5. Chang, F. C., and Swenson, R. P. (1997) Regulation of oxidation−reduction potentials through redox-linked ionization in the Y98H mutant of the *Desulfovibrio vulgaris* [Hildenborough] flavodoxin: Direct proton nuclear magnetic resonance spectroscopic evidence for the redox-dependent shift in the pK_a of Histidine-98, *Biochemistry 36*, 9013−9021.
6. Walsh, M. A., McCarthy, A., O'Farrell, P. A, McArdle, P., Cunningham, P. D., Mayhew, S. G., and Higgins, T. M. (1998) X-ray crystal structure of the *Desulfovibrio vulgaris* (Hildenborough) apoflavodoxin−riboflavin complex, *Eur. J. Biochem. 258*, 362−371.
7. Hoover, D. M., Drennan, C. L., Metzger, A. L., Osborne, C., Weber, C. H., Pattridge, K. A., and Ludwig, M. L. (1999) Comparisons of wild-type and mutant flavodoxins from *Anacystis nidulans*. Structural determinants of the redox potentials, *J. Mol. Biol. 294*, 725−743.
8. Geoghegan, S. M., Mayhew, S. G., Yalloway, G. N., and Butler, G. (2000) Cloning, sequencing, and expression of the gene for flavodoxin from *Megasphaera elsdenii* and the effects of removing the protein negative charge that is closest to N(1) of the bound FMN, *Eur. J. Biochem. 267*, 4434−4444.
9. McCarthy, A. A., Walsh, M. A., Verma, C. S., O'Connell, D. P., Reinhold, M., Yalloway, G. N, D'Arcy, D., Higgins, T. M, Voordouw, G., and Mayhew, S. G. (2002) Crystallographic investigation of the role of aspartate 95 in the modulation of the redox potentials of *Desulfovibrio vulgaris* flavodoxin, *Biochemistry 41*, 10950−10962.
10. Zhou, Z., and Swenson, R. P. (1996) The cumulative electrostatic effect of aromatic stacking interactions and the negative electrostatic environment of the flavin mononucleotide binding site is a major determinant of the reduction potential for the flavodoxin from *Desulfovibrio vulgaris* [Hildenborough], *Biochemistry 35*, 15980−15988.
11. Lostao, A., Gomez-Moreno, C., Mayhew, S. G., and Sancho, J. (1997) Differential stabilization of the three FMN redox forms by tyrosine 94 and tryptophan 57 in flavodoxin from *Anabaena* and its influence on the redox potentials, *Biochemistry 36*, 14334−14344.

12. Druhan, L. J., and Swenson, R. P. (1998) Role of methionine 56 in the control of the oxidation−reduction potentials of the *Clostridium beijerinckii* flavodoxin: Effects of substitutions by aliphatic amino acids and evidence for a role of sulfur−flavin interactions, *Biochemistry 37*, 9668−9678.
13. Bradley, L. H., and Swenson, R. P. (1999) Role of glutamate-59 hydrogen bonded to N(3)H of the flavin mononucleotide cofactor in the modulation of the redox potentials of the *Clostridium beijerinckii* flavodoxin. Glutamate-59 is not responsible for the pH dependency but contributes to the stabilization of the flavin semiquinone, *Biochemistry 38*, 12377−12386.
14. Bradley, L. H., and Swenson, R. P. (2001) Role of hydrogen bonding interactions to N(3)H of the flavin mononucleotide cofactor in the modulation of the redox potentials of the *Clostridium beijerinckii* flavodoxin, *Biochemistry 40*, 8686−8695.
15. Ludwig, M. L., Pattridge, K. A., Metzger, A. L., Dixon, M. M., Eren, M., Feng, Y., and Swenson, R. P. (1997) Control of oxidation−reduction potentials in flavodoxin from *Clostridium beijerinckii:* The role of conformation changes, *Biochemistry 36*, 1259−1280.
16. Chang, F. C., and Swenson, R. P. (1999) The midpoint potentials for the oxidized-semiquinone couple for Gly57 mutants of the *Clostridium beijerinckii* flavodoxin correlate with changes in the hydrogen-bonding interaction with the proton on N(5) of the reduced flavin mononucleotide cofactor as measured by NMR chemical shift temperature dependencies. *Biochemistry 38*, 7168−7176.
17. O′Farrell, P. A., Walsh, M. A., McCarthy, A. A., Higgins, T. M., Voordouw, G., and Mayhew, S. G. (1998) Modulation of the redox potentials of FMN in *Desulfovibrio vulgaris* flavodoxin: Thermodynamic properties and crystal structures of glycine-61 mutants, *Biochemistry 37*, 8405−8416.
18. Smith, W. W., Pattridge, K. A., Ludwig, M. L., Petsko, G. A., Tsernoglou, D., Tanaka, M., and Yasunobu, K. T. (1983) Structure of oxidized flavodoxin from *Anacystis nidulans*, *J. Mol. Biol*. *165*, 737−753.
19. Fukuyama, K., Wakabayashi, S., Matsubara, H., and Rogers, L. J. (1990) Tertiary structure of oxidized flavodoxin from an eukaryotic red alga *Chondrus crispus* at 2.35 Å resolution. Localization of charged residues and implication for interaction with electron-transfer partners, *J. Biol. Chem*. *265*, 15804−15812.
20. Burkhart, B., Ramakrisman, B., Yan, H., Reedstrom, R., Markley, J., Straus, N., and Sundaralingam, M. (1995) Structure of the trigonal form of recombinant oxidized flavodoxin from *Anabaena* 710 at 1.4 Å resolution, *Acta Crystallogr*., *Sect. D 51*, 318−330.
21. Rao, S., Shaffie, F., Yu, C., Satyshur, K., Stokman, B., Markley, J. L., and Sundarlingam, M. (1992) Structure of the oxidized long-chain flavodoxin fom Anabaena 7120 at 2 Å resolution, *Protein Sci. 1*, 1413−1427.
22. Watenpaugh, K. D., Sieker, L. C., and Jensen, L. H. (1973) The binding of riboflavin-5′-phosphate in a flavoprotein: Flavodoxin at 2.0 Å resolution, *Proc. Natl. Acad. Sci. U.S.A. 70*, 3857−3860.
23. Watt, W., Tulinski, A., Swenson, R. P., and Watenpaugh, K. D. (1991) Comparison of the crystal structures of a flavodoxin in its three oxidation states at cryogenic temperatures, *J. Mol. Biol*. *218*, 195−208.
24. Smith, W. W., Burnett, R. M., Darling, G. D., and Ludwig, M. L. (1977) Structure of the semiquinone form of flavodoxin from *Clostridum MP*. Extension of 1.8 Å resolution and some comparisons with the oxidized state, *J. Mol. Biol. 117*, 195−225.
25. Sharkey, C. T., Mayhew, S. G., Higgins, T. M., and Walsh, M. A. (1997) Crystallographic studies on flavodoxin from *Megasphaera eldenii*, in *Flavins and Flavoproteins* (Stephenson, K. J., Massey, V., and Williams, C. H., Jr., Eds.) pp 445−448, University of Calgary Press, Calgary, Canada.
26. Romero, A., Caldeira, J., Legall, J., Moura, I., Moura, J. J., and Romao, M. J. (1996) Crystal structure of flavodoxin from *Desulfovibrio desulfuricans* ATCC 27774 in two oxidation states, *Eur. J. Biochem. 239*, 190−196.
27. Reynolds, R. A., Watt, W., and Watenpaugh, K. D. (2001) Structures and comparison of the Y98H (2.0 Å) and Y98W (1.5 Å) mutants of flavodoxin (*Desulfovibrio vulgaris*), *Acta Crystallogr., Sect. D 57*, 527−535.
28. Lostao, A., El Harrous, M., Daoudi, F., Romero, A., Parody-Morreales, A., and Sancho, J. (2000) Dissecting the energetics of the apoflavodoxin−FMN complex, *J. Biol. Chem. 275*, 9518−9516.
29. Lostao, A., Daoudi, F., Irún, M. P., Ramón, A., Fernández-Cabrera, C., Romero, A., Sancho, J. (2003) How FMN binds to *Anabaena* apoflavodoxin: A hydrophobic encounter at an open binding site, *J. Biol. Chem. 278*, 24053−24061.
30. Genzor, C. G., Perales-Alcon, A., Sancho, J., and Romero, A. (1996) Closure of a tyrosine/tryptophan aromatic gate leads to a compact fold in apo flavodoxin, *Nat. Struct. Biol. 3*, 329−332.
31. Helms, L. R., and Swenson, R. P. (1991) Cloning and characterization of the flavodoxin gene from *Desulfovibrio desulfuricans*, *Biochim. Biophys. Acta 1089*, 417−419.
32. Helms, L. R., and Swenson, R. P. (1992) The primary structures of the flavodoxins from two strains of *Desulfovibrio gigas.* Cloning and nucleotide sequence of the structural genes, *Biochim. Biophys. Acta 1131*, 325−328.
33. Helms, L. R., Krey, G. D., and Swenson, R. P. (1990) Identification, sequence determination, and expression of the flavodoxin gene from *Desulfovibrio salexigens*, *Biochem. Biophys. Res. Commun*. *168*, 809−817.
34. Kasim, M., and Swenson, R. P. (2001) Alanine-scanning of the 50's loop in the *Clostridium beijerinckii* flavodoxin: Evaluation of additivity and the importance of interactions provided by the main chain in the modulation of the oxidation−reduction potentials, *Biochemistry 40*, 13548−13555.
35. Fukuyama, K., Matsubara, H., and Rogers, L. J. (1992) Crystal structure of oxidized flavodoxin from a red alga *Chondrus crispus* refined at 1.8 Å resolution. Description of the flavin mononucleotide binding site, *J. Mol. Biol*. *225*, 775−789.
36. Irún, M. P., García-Mira, M. M., Sanchez-Ruiz, J. M., and Sancho, J. (2001) Native hydrogen bonds in a molten globule the Apoflavodoxin thermal intermediate, *J. Mol. Biol*. *306*, 877−888.
37. Edmondson, D. E., and Tollin, G. (1971) Chemical and physical characterization of the Shethna flavoprotein and apoprotein and kinetics and thermodynamics of flavin analog binding to the apoprotein, *Biochemistry 10*, 124−132.
38. Mayhew, S. G., and Massey, V. (1969) Purification and characterization of flavodoxin from *Peptostreptococcus elsdenii*, *J. Biol. Chem*. *244*, 794−802.
39. Medina, M., Lostao, A., Sancho, J., Gómez-Moreno, C., Cammack, R., Alonso, P. J., and Martínez, J. (1999) Electron−nuclear double resonance and hyperfine sublevel correlation spectroscopic studies of flavodoxin mutants from *Anabaena* sp. PCC7119, *Biophys. J. 77*, 1712−1720.
40. Martínez, J. I., Alonso, P. J., Gómez-Moreno, C., and Medina, M. (1997) One- and two-dimensional ESEEM spectroscopy of flavoproteins, *Biochemistry 36*, 15526−15537.
41. Mayhew, S. G. (1999) Potentiometric measurement of oxidation−reduction potentials, in *Flavoprotein Protocols* (Chapman, S. K., and Reid, G. A., Eds.) pp 49−59, Humana Press, Totowa, NJ.
42. Guex, N., and Peitsch, M. C. (1997) SWISS-MODEL and the Swiss-PdbViewer: An environment for comparative protein modeling, *Electrophoresis 18*, 2714−2723.
43. Pueyo, J. J., Gomez-Moreno, C., and Mayhew, S. G. (1991) Oxidation−reduction potencials of ferredoxin−$NADP^+$ oxidoreductase and flavodoxin from *Anabaena* PCC7119 and their electrostatic complexes, *Eur. J. Biochem. 202*, 1065−1071.
44. Yalloway, G. N., Mayhew, S. G., Malthouse, J. P., Gallagher, M. E., and Curley, G. P. (1999) pH-dependent spectroscopic changes associated with the hydroquinone of FMN in flavodoxins, *Biochemistry 38*, 3753−3762.
45. Yalloway, G. N., Mayhew, S. G., Boren, S. J. and Vervoort, J. (1999) Effects of pH on the ^{13}C and ^{15}N NMR spectra of the hydroquinone of *Desulfovibrio vulgaris* flavodoxin and its G61A mutant, in *Flavins and Flavoproteins* (Ghisla, S., Kroneck, P., Macheroux, P., and Sund, H., Eds.) pp 187−190, Rudolf Weber, Berlin, Germany.
46. Gast, R., Valk, B. E., Muller, F., Mayhew, S. G., and Veeger, C. (1976) Studies on the binding of FMN by apoflavodoxin from *Peptostreptococcus elsdenii*, pH and NaCl concentration dependence, *Biochim. Biophys. Acta 28*, 463−471.
47. Curley, G. P., Carr, M. C., Mayhew, S. G., and Voordouw, G. (1991) Redox and flavin-binding properties of recombinant flavodoxin from *Desulfovibrio vulgaris*, *Eur. J. Biochem. 202*, 1091−1100.
48. Murray, A., and Swenson, R. P. (2003) Mechanism of flavin mononucleotide cofactor binding to the *Desulfovibrio vulgaris* flavodoxin. 1. Kinetic evidence for cooperative effects associated with the binding of inorganic phosphate and the 5′-phosphate moiety of the cofactor, *Biochemistry 42*, 2307−2316.
49. Franken, H. D., Rüterjans, H., and Müller, F. (1984) Nuclear magnetic resonance investigation of ^{15}N-labeled flavins, free and

bound to *Megasphaera elsdenii* apoflavodoxin, *Eur. J. Biochem. 138*, 481−489.
50. Ludwig, M. L., Schopfer, L. M., Metzger, A. L., Pattridge, K. A., and Massey, V. (1990) Structure and oxidation−reduction behavior of 1-deaza-FMN flavodoxins: Modulation of redox potentials in flavodoxins, *Biochemistry 29*, 10364−10375.
51. Feng, Y., and Swenson, R. P. (1997) Evaluation of the role of specific acidic amino acid residues in electron transfer between the flavodoxin and cytochrome *c*3 from *Desulfovibrio vulgaris*, *Biochemistry 36*, 13617−13628.
52. Moonen, C. T. W., Vervoort, J., and Müller, F. (1984) Some new ideas about the possible regulation of redox potentials in flavoproteins, with special reference to flavodoxin, in *Flavins and Flavoproteins* (Bray, R. C., Engel, P. C, and Mayhew, S. G., Eds.) pp 493−496, De Guyter, Berlin, Germany.
53. Casaus, J. L., Navarro, J. A., Hervas, M., Lostao, A., De la Rosa, M. A., Gómez-Moreno, C., Sancho, J., and Medina, M. (2002). *Anabaena* sp. PCC7119 flavodoxin as electron carrier from photosystem I to ferredoxin−$NADP^+$ reductase. Role of Trp(57) and Tyr(94), *J. Biol. Chem. 277*, 22338−22344.
54. Draper, R. D., and Ingraham, L. L. (1968) A potentiometric study of the flavin semiquinone equilibrium, *Arch. Biochem. Biophys.* 125, 802−808.
55. Mayhew, S. G. (1999) The effects of pH and semiquinone formation on the oxidation−reduction potentials of flavin mononucleotide, *Eur. J. Biochem. 265*, 698−702.
56. Wallace, A. C., Laskowski, R. A., and Thornton, J. M. (1995) LIGPLOT: A program to generate schematic diagrams of protein−ligand interactions, *Protein Eng. 8*, 127−134.
57. DeLano, W. L. (2002) The PyMol molecular graphics system, DeLano Scientific, San Carlos, CA.

BI0483256